ELSEVIER

Since January 2020 Elsevier has created a COVID-19 resource centre with free information in English and Mandarin on the novel coronavirus COVID-19. The COVID-19 resource centre is hosted on Elsevier Connect, the company's public news and information website.

Construction, expression and antiviral activity analysis of recombinant adenovirus expressing human IFITM3 *in vitro*

Shouwen Du [a,c,1], Yinyue Jiang [a,1], Wang Xu [a], Jieying Bai [a], Mingyao Tian [a], Maopeng Wang [a], Yuhang Wang [c], Tingting Cao [a], Lina Song [a], Yuhang Jiang [a], Jing Chen [a], Tingting Fu [a], Penfeng Hao [a], Tiyuan Li [c], Shipin Wu [c], Linzhu Ren [b,*], Ningyi Jin [a,*], Chang Li [a,*]

[a] *Key Laboratory of Jilin Province for Zoonosis Prevention and Control, Military Veterinary Institute, Academy of Military Medical Sciences, Changchun 130112, China*
[b] *Jilin Provincial Key Laboratory of Animal Embryo Engineering, College of Animal Sciences, Jilin University, Changchun 130062, China*
[c] *2nd Clinical Medical College of Jinan University, Shenzhen People's Hospital, Shenzhen 518020, China*

ABSTRACT

Interferon-inducible transmembrane protein 3 (IFITM3) inhibits the replication of multiple pathogenic viruses by blocking their entry. In this study, we constructed a shuttle plasmid, harboring human IFITM3. Thereafter, recombinant adenovirus rAd5-IFITM3 was obtained by co-transfection of the linearized viral backbone vector pAd5 and the shuttle plasmid. The results showed that human IFITM3 did not affect the assembly and morphogenesis of progeny adenovirus. Human IFITM3 can be expressed in both A549 and MDCK cells in a time dependent manner. Furthermore, cells infected with rAd5-IFITM3 at a multiplicity of infection (MOI) of 100 for 24 h were challenged with avian influenza virus (AIV) H5N1 at an MOI of 1 for 6, 12 and 24 h. Rates of H5N1 infection in rAd5-IFITM3 cells were significantly decreased at 24 h post-infection (hpi), in a time dependent manner, compared with that of wild type wtAd5-infected cells. The expressions of viral genes were significantly inhibited at transcriptional and translational levels at 6 and 12 hpi. These results suggest that IFITM3 can suppress H5N1 replication in the early stage of the infection, which may be used as a promise agent against H5N1 infection *in vivo*.

© 2019 Elsevier B.V. All rights reserved.

1. Introduction

Recombinant adenovirus, as an effective *in vivo* and *in vitro* gene delivery vector, is widely used in cancer therapy, gene therapy and vaccine expressing foreign antigen [1–5]. The recombinant adenovirus rescued by transfecting adenovirus vectors into HEK293 cells are replication defective, with certain essential viral genes are replaced by a foreign gene [1,6], and the recombinant adenovirus can efficiently accommodate a larger foreign gene (up to 37 kb of foreign gene) and infect almost all types of cells and tissues [6–8]. Therefore, to date, replication-defective recombinant Ad5 vectors have been considered as potential vaccine delivery vehicles for human immunodeficiency virus (HIV)-1, hepatitis C virus (HCV), influenza virus, and other viruses [9–12].

The interferon-induced transmembrane proteins (IFITMs) are a family of small membrane proteins, which was induced by type I and II interferon and expressed broadly in tissues and cell lines [13–15]. IFITMs have diverse roles, including the control of cell proliferation, promotion of homotypic cell adhesion, protection against viral infection,

promotion of bone matrix maturation and mineralization, and mediating germ cell development [16]. Recently, IFITMs were identified as broad-spectrum antiviral proteins by inhibiting the early step of virus infection, however different IFITMs has different antiviral activity [17–21]. Furthermore, there is almost no species specificity in antiviral activity of IFITMs [22,23]. For example, primate-derived IFITMs are effective inhibitors of simian immunodeficiency virus (SIV), and primate IFITM3 alleles also exhibit superior anti-HIV activity compared to human IFITM3 [22,24,25]. Amino-terminal mutants of primate IFITM3 are more easily incorporated into HIV virions, resulting in enhanced inhibition of HIV-1 fusion [25]. Among the IFITMs, IFITM3 was widely studied for its wide range of effective antiviral activities, which could restrict Dengue virus, SARS coronavirus, Ebola virus, HCV, influenza A virus, Zika virus, West Nile virus, and so on [26–30]. We also discovered that overexpression of human IFITM3 significantly restricted vaccinia virus infection, replication and proliferation, mainly by interfering with virus entry in a low pH-dependent manner [18].

We previously found that A549 cell stably expressing human IFITM3 displayed strong restriction effect on avian influenza virus (AIV) H5N1 infection [23]. Therefore, whether IFITM3 can be used as an antiviral agent expressed by recombinant adenovirus needs to be elucidated. In the present study, human IFITM3 was inserted into replication-defective recombinant Ad5 vectors, followed by the rescuing the

recombinant adenovirus expressing the human IFITM3. And *in-vitro* antiviral efficacy of the recombinant adenovirus was evaluated against influenza virus H5N1 challenge.

2. Materials and methods

2.1. Virus and cells

Avian influenza virus (AIV) H5N1 (A/chicken/Jilin/9/2004(H5N1)) was kindly provided by Professor Ningyi Jin.

Human embryonic kidney 293 (HEK293), human lung adenocarcinoma A549 cell (A549) and Madin-Darby canine kidney epithelial cell (MDCK) were stored in our lab.

2.2. Plasmid construction

The plasmid pLV-IFITM3 was constructed previously, which contained human IFITM3 gene [18,23]. The viral backbone plasmid pacAd5 9.2-100 (pacAd5) and shuttle plasmid pacAd5 CMVK-NpA (pacAd5 CMV) were kindly provided by Professor Ningyi Jin.

The plasmids pLV-IFITM3 and pacAd5 CMV were digested by *Eco*R I and *Bam*H I, respectively, and a 420 bp of human IFITM3 (hIFITM3) gene and a 6200 bp of linearized pacAd5 CMV were purified. Then, two fragments were linked with T4 DNA ligase to generate shuttle plasmid pacAd-IFITM3. The shuttle plasmid pacAd-IFITM3 was identified by digestion with *Eco*R I and *Bam*H I and sequencing analysis.

2.3. Preparation of recombinant adenovirus

Two-plasmid transfection system was used to generate recombinant adenovirus particles, including the shuttle plasmid and the viral backbone plasmid. Briefly, the viral backbone vector pacAd5 and shuttle plasmid pacAd-IFITM3 were linearized by *Pac* I and *Nhe* I, and purified, respectively. HEK293 cells (4×10^5/well) were cultured on 6-well plate and incubated at 37 °C in a 5% CO_2 atmosphere for 24 h. The cells were co-transfected with the linearized viral backbone vector
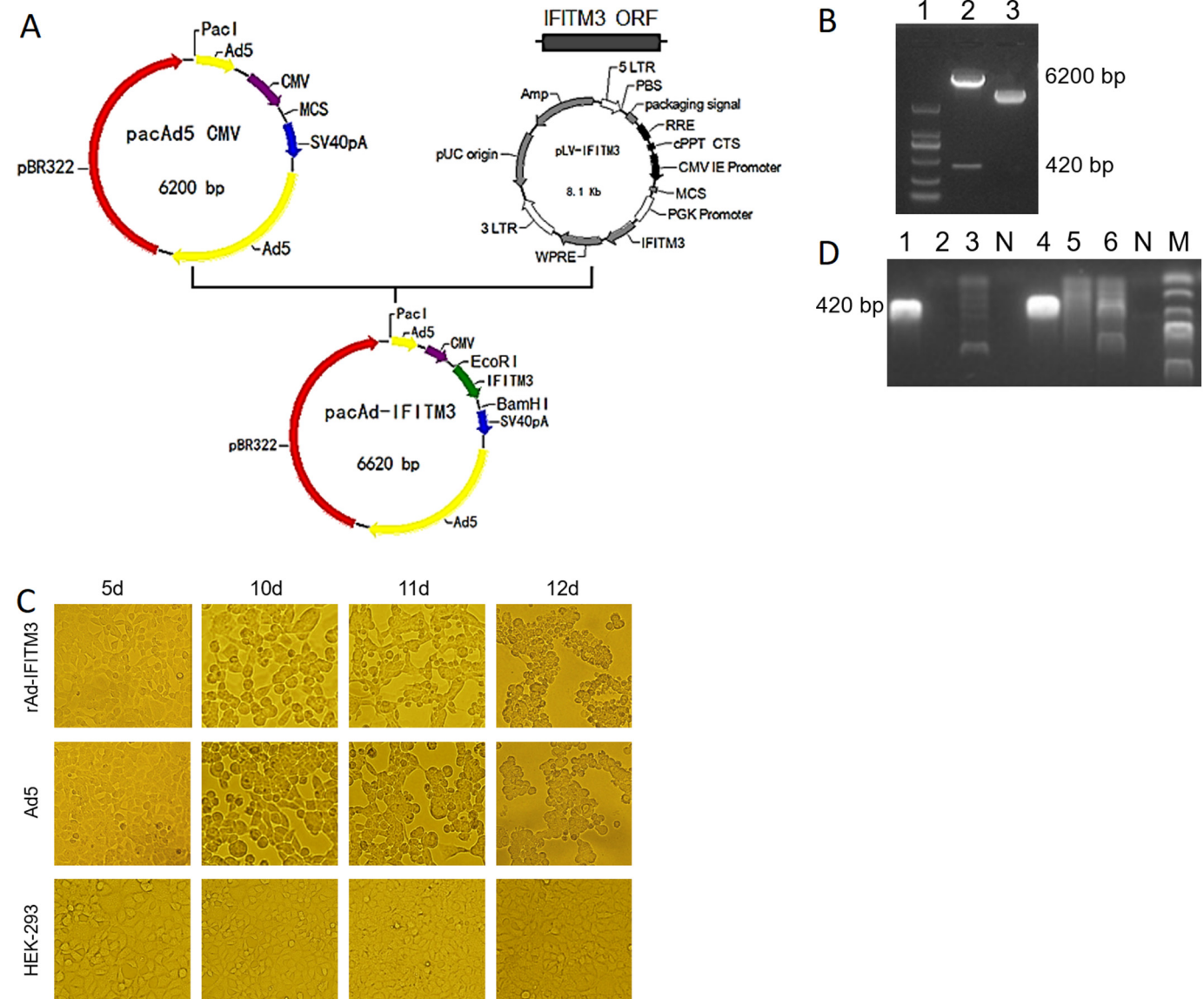

Fig. 1. Construction and identification of recombinant adenovirus. (a) Schematic diagram of recombinant plasmid. (b) Enzyme digestion of pacAd-IFITM3. 1, DL2000 DNA Marker; 2, pacAd-IFITM3 digested with *Eco*R I and *Bam*H I; 3, pacAd-IFITM3. (c) Cytopathic effects after transfection. HEK293 cell was co-transfected with the linearized viral backbone vector pacAd5 and shuttle pacAd-IFITM3 (3:1) using X-tremeGENE HP DNA Transfection Reagent. The transfected cells were monitored for CPE at 5, 10, 11, and 12 days after transfection. The progeny virus was collected and designated as rAd5-IFITM3. The viral backbone vector pacAd5 and shuttle plasmid pacAd5 CMV were linearized and co-transfected in HEK293 cell to produce wild type adenovirus wtAd5. (d) PCR results of rAd5-IFITM3 and wtAd5. 1, HEK-293 supernatants of rAd5-IFITM3; 2, HEK-293 supernatants of wtAd5; 3, HEK-293 supernatants (control); 4, HEK-293 cell lysis of rAd5-IFITM3; 5, HEK-293 cell lysis of wtAd5; 6, HEK-293 cell lysis (control); M, DL2000 DNA Marker; N, negative control.

pacAd5 and shuttle pacAd-IFITM3 (3:1) using X-tremeGENE HP DNA Transfection Reagent according to the manufacture's instruction (Roche). Transfected cells were monitored for cytopathic effects (CPE) and collected 20 days after transfection. Then, the cells were lysed for three cycles of freeze and thaw, and centrifuged at 3000 rpm for 10 min. The virus was collected from the supernatant and designated as rAd5-IFITM3. At the same time, the viral backbone vector pacAd5 and shuttle plasmid pacAd5 CMV were linearized and co-transfected in HEK293 cell to produce wild type adenovirus wtAd5.

2.4. PCR, RT-PCR and real time PCR

For gene identification, viral genomic DNA was extracted from the virus infected HEK293 cells using TIANamp Virus DNA/RNA Kit according to the manufacturer's protocol (Tiangen Biotech Co., LTD, Beijing, China). PCR was performed using 2 × Taq PCR MasterMix (Tiangen Biotech Co., LTD, Beijing, China) with primers targeting human IFITM3 (Fp3: 5′-GAATTCGCCACCATGGATTAC AAGGATGACGACGATAAGAAT CACACTGTCCAAAC-3′; Rp3: 5′-GGATCCCTATCCATAGGC CTGGAAGA-3′) described previously [23]. The PCR products were analyzed on 1% agarose gel containing 0.5 g/mL ethidium bromide (EB). The experiments were repeated at least three times.

For gene expression, total RNA was extracted from the virus infected cells using TRNzol-A+ Reagent and reverse transcribed using the BioRT cDNA First Strand Synthesis Kit (Bioer, China) according to the manufacturer's instructions. PCR was performed using primers targeting human IFITM3 (primers Fp3 and Rp3). Real time PCR was performed
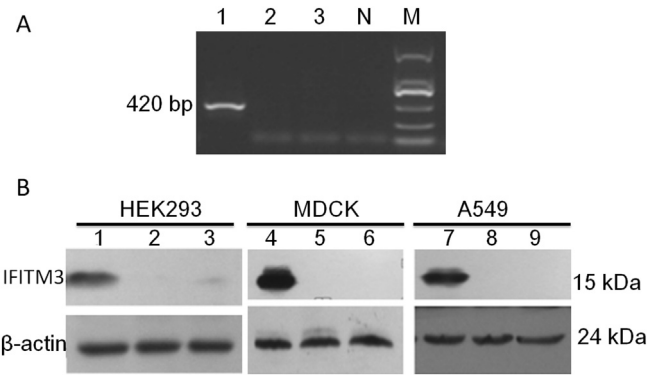

Fig. 3. Expression of human IFITM3 in HEK293 cell. (a) RT-PCR of virus infected HEK293 cell. 1, rAd5-IFITM3; 2, wtAd5; 3, mock infected HEK293 cell; N, negative control; M, DL2000 DNA Marker. (b) Western blot of adenovirus infected HEK293, MDCK and A549 cells. Western blot was performed using Mouse polyclonal anti-IFITM3 antibody (1:1000, Proteintech, USA) or Mouse monoclonal anti-β-actin antibody (1:1000, Beyotime, China) as primary antibody and HRP- conjugated goat anti-mouse IgG (1:2000, Beyotime, China) as secondary antibodies. β-Actin was used as control. 1, 4, 7, rAd5-IFITM3; 2, 5, 8, wtAd5; 3, 6, 9, mock infected.

using GoTaq qPCR Master Mix (Promega, USA) with primers targeting human IFITM3 (qFp3: 5′-ATGTCGTCTGGTCCCTGTTC-3′; qRp3: 5′-GTCATGAGGATGCCCAGAAT-3′), H5N1 M2 gene (F: CTCTTGTTGCCACA AGTAT; R: TCCGTAGAAGGCCCTCTTTTC) and GAPDH (qFp: 5′-ACCCAC TCCTCCACCTTTG AC-3′; qRp:5′-TGTTGCTGTAGCCAAATTCGTT-3′), respectively, described previously [18,23].

2.5. Protein preparation and western blot

To obtain total protein, HEK293 cells were infected with wtAd5 or rAd5-IFITM3 for 48 h. The cells were collected and centrifuged at 4 °C, 3000 rpm for 10 min. The cell pellet was incubated with chilled RIPA lysis buffer (Beyotime, China) for 15 min, ultrasonicated for15 s, 15 times, on ice. The homogenates were centrifuged at 4 °C, 12000 rpm for 2 min. Supernatant was collected and analyzed using western blot.

The membrane and cytoplasmic proteins were extracted using Membrane and Cytosol Protein Extraction Kit (Beyotime, China) according to the protocol described in the manufacture's instruction.

For western blot, protein was separated with 12% sodium dodecyl sulfate-polyacrylamide gel electrophoresis (SDS-PAGE) and transferred onto nitrocellulose membrane. Membranes were washed with Tris-buffered saline Tween-20 (TBST) once and blocked in blocking buffer consisting of 5% non-fat milk for 1 h. Primary antibody was incubated with the membrane, followed by three times wash with TBST. Membranes were incubated with horseradish peroxidase (HRP)-conjugated secondary antibodies for 1 h and then washed for three times. The results were visualized with the enhanced chemoluminescence (ECL) plus kit (Thermo, USA).
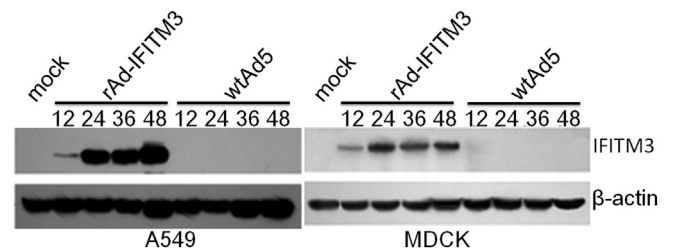

Fig. 2. Morphology of recombinant adenovirus rAd5-IFITM3 (a) and wild type adenovirus wtAd5 (b) (40K×).

Fig. 4. Expression of human IFITM3 was increased in a time dependent manner in the cells. Western blot was performed using Mouse polyclonal anti-IFITM3 antibody (1:1000, Proteintech, USA) or Mouse monoclonal anti-β-actin antibody (1:1000, Beyotime, China) as primary antibody and HRP- conjugated goat anti-mouse IgG (1:2000, Beyotime, China) as secondary antibodies. β-Actin was used as control.

Fig. 5. Distribution of human IFITM3 in A549 and MDCK cells. Western blot was performed using Mouse polyclonal anti-IFITM3 antibody (1:1000, Proteintech, USA) or Mouse monoclonal anti-β-actin antibody (1:1000, Beyotime, China) as primary antibody and HRP- conjugated goat anti-mouse IgG (1:2000, Beyotime, China) as secondary antibodies. β-Actin was used as control. M, cell membrane; C, cytoplasm. Mock, negative control.
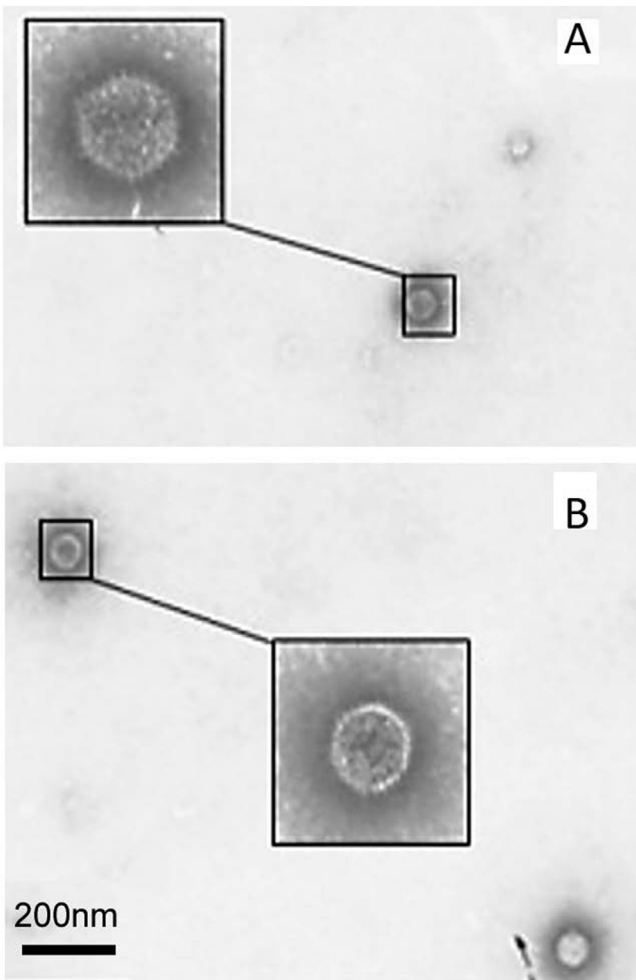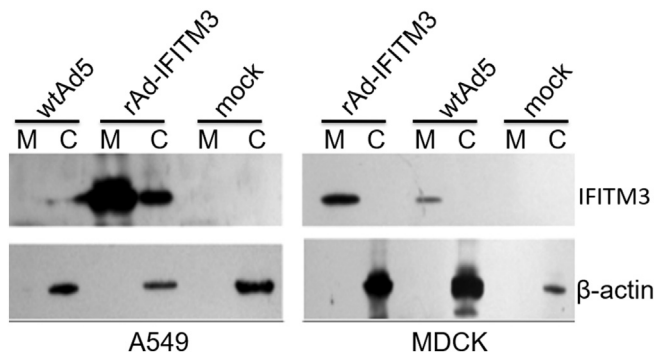
2.6. Virus titration

For virus titration, 5×10^3 of HEK293 cells were plated into 96-well plate and cultured at 37 °C in a 5% CO_2 atmosphere for 12–24 h. The viruses were 10-fold serially diluted from 10^{-1} to 10^{-11} in DMEM medium and added into the well at 37 °C, 5% CO_2. 4 h post infection (hpi), 200 μL of DMEM supplemented with 10% Fetal bovine serum (FBS) was added into the well and the cells were cultured at 37 °C in a 5% CO_2 atmosphere for 4–7 d. The CPE was monitored and virus titer (50% tissue culture infective dose, $TCID_{50}$) was calculated according to the protocol described by Reed-Muench.

2.7. Transmission electron microscopy

For examinations of viruses by transmission electron microscopy, the recombinant adenovirus was incubated in PBS containing 2% glutaric acid at 40 °C for 24 h. then, the virus was absorbed on the grid, washed with distill water for three times, and negatively stained with 2% Phosphotungstic Acid (pH 6.5). Subsequently, the virus was

examined with a JEM 1200 EX II transmission electron microscope (JEOL USA, Peabody, MA, USA).

2.8. MTS assay

The inhibitory effect of adenovirus on MDCK and A549 cells was detected using MTS assay. Briefly, 100 μL of cells (5×10^3 cells/well) were plated into 96-well plate at 37 °C, 5% CO_2 for 12 to 24 h. The cells were infected with 100 μL of rAd5-IFITM3 or wtAd5 at different multiplicity of infection (MOI = 1, 10, 100 and 1000), respectively. 12, 24, 36 and 48 hpi, cells were incubated with 20 μL of MTS solution at 37 °C, 5% CO_2 for 1 h, and the absorbance at 490 nm was measured. The data were calculated from the mean of six replicates.

To evaluate the cytopathic effect of H5N1 on MDCK and A549 cells, 100 μL of cells (5×10^3 cells/well) were plated into 96-well plate at 37 °C, 5% CO_2 for 12 to 24 h. The cells were infected with 100 μL of rAd5-IFITM3 or wtAd5 at MOI of 100, respectively. 24 hpi, cells were infected with influenza virus H5N1 at different MOI (MOI = 0, 1, 10 and 100). 12, 24, 36 and 48 hpi, cells were incubated with 20 μL of MTS solution at 37 °C, 5% CO_2 for 1 h, and the absorbance at 490 nm was measured. The data were calculated from the mean of six replicates. Inhibitory rate was calculated as (OD_{490} of control − OD_{490} of treatment) / OD_{490} of control × 100%.

2.9. Statistical analysis

Statistical analysis was performed using Spss17.0 statistical software. Data are presented as the mean ± standard deviation (SD). Differences with a P-value < 0.05 were considered as statistically significant.

3. Results

3.1. Recombinant adenovirus expressing human IFITM3 was obtained

To construct a shuttle plasmid, the plasmids pLV-IFITM3 and pacAd5 CMV were digested by *Eco*R I and *Bam*H I, respectively, and a 420 bp of human IFITM3 (hIFITM3) gene and a 6200 bp of linearized pacAd5 CMV were purified, followed by the ligation of the hIFITM3 gene and the linearized pacAd5 CMV (Fig. 1a). The resulting shuttle plasmid was identified
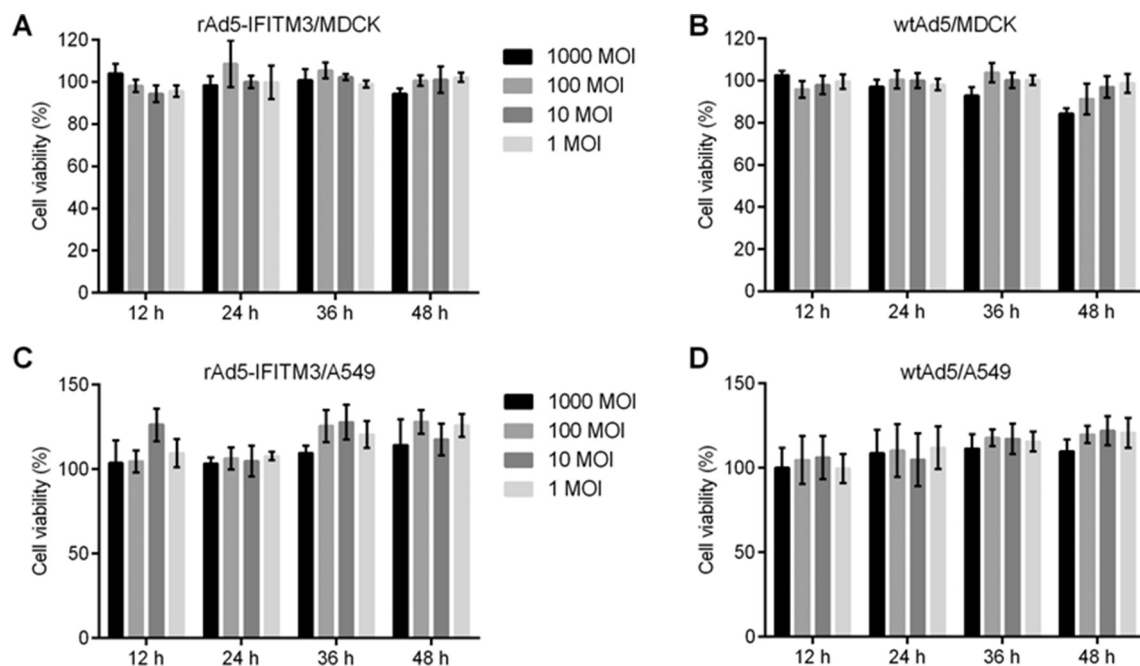

Fig. 6. Inhibitory rate of rAd5-IFITM3 on A549 and MDCK cells. A549 and MDCK cells were infected with rAd5-IFITM3 or wtAd5 at different MOI (1, 10, 100 and 1000). The inhibition rates of cell growth were calculated using MTS at 12, 24, 36 and 48 hpi.

by digestion with *Eco*R I and *Bam*H I and designated as pacAd-IFITM3 (Fig. 1b). The results of restriction analysis showed that plasmid pacAd-IFITM3 (Fig. 1b) was constructed successfully. Furthermore, the plasmid was also confirmed by DNA sequencing analysis (data not shown).

To obtain recombinant adenovirus, viral backbone vector pacAd5 and shuttle pacAd-IFITM3 were linearized by *Pac* I and *Nhe* I, respectively, and co-transfected into HEK293 cell using X-tremeGENE HP DNA Transfection Reagent. Due to the pacAd5 and pacAd-IFITM3 encoded genes and elements required for proper packaging and production of adenovirus, therefore, the recombinant adenovirus can be obtained from HEK293 cells. The resulting recombinant adenovirus was designated as rAd5-IFITM3. The backbone vector pacAd5 and shuttle plasmid pacAd5 CMV were linearized by *Pac* I, respectively, and co-transfected into HEK293 cell to generate wild type adenovirus wtAd5. The results showed that obvious CPE were observed on the 10 days after co-transfection, with the cells rounded up and clumped together obviously, empty areas became visible and a remarkable decrease in live cells was observed on the 11th and 12th after co-transfection (Fig. 1c), indicating adenoviruses, wtAd5 and rAd5-IFITM3, were obtained successfully.

To further confirm these results, viral genomic DNA was extracted from the supernatant and cell lysis, and amplified by PCR. The results showed that 420 bp of human IFITM3 were amplified from supernatants and cell lysis of rAd5-IFITM3 (Fig. 1d, lane 1 and 4), while no specific band can be detected in the other groups (Fig. 1d). These results indicated that human IFITM3 was integrated into the recombinant rAd5-IFITM3.

In addition, virus titers were evaluated to analyze viral proliferation. The virus titer of rAd5-IFITM3 was up to 4.68×10^9/mL (TCID$_{50}$), which was similar to that of wtAd5, as the titer of the later was 4.0×10^9/mL (TCID$_{50}$). These results demonstrated that the expression of exogenous genes did not affect the production of adenovirus.

To view the virions, the viruses were negatively stained and examined using transmission electron microscopy. The results showed that typical adenoviruses were observed, with non-enveloped and the diameters of approximately 90 nm (Fig. 2). As shown in Fig. 2, the shape of rAd5-IFITM3 (Fig. 2a) was similar with that of wtAd5 (Fig. 2b). These results indicated that expression of human IFITM3 did not affect the viral morphogenesis.
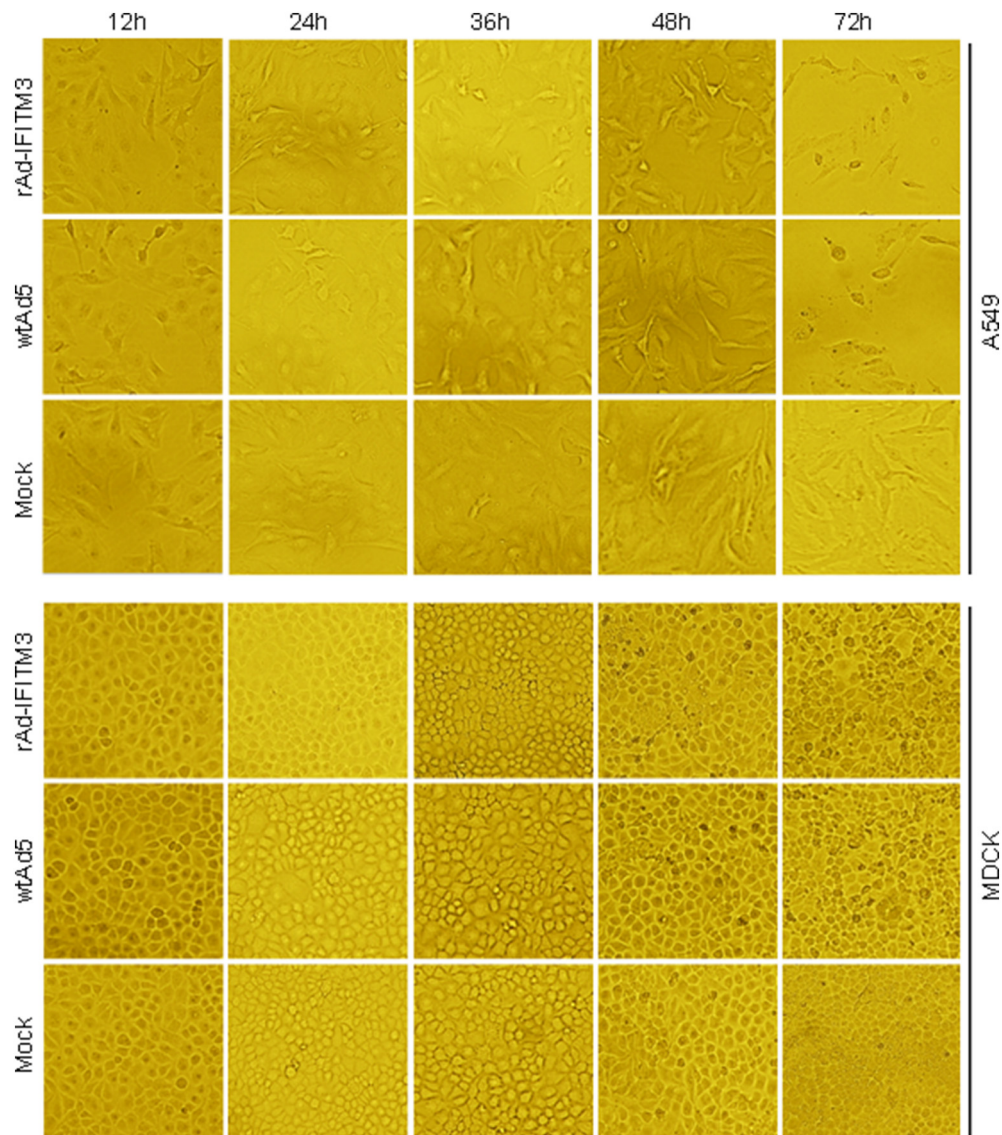

Fig. 7. CPE of adenovirus on A549 and MDCK cells (200×). A549 and MDCK cells were infected or mock infected with rAd5-IFITM3 or wtAd5 at MOI of 100. CPE was observed using microscope at 12, 24, 36, 48 and 72 hpi.
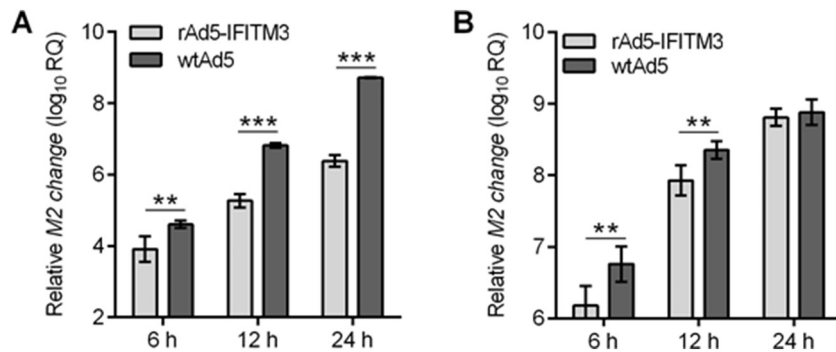
Fig. 8. qPCR analysis. Cells were infected or mock-infected with rAd5-IFITM3 or wtAd5 at an MOI of 100 for 24 h, followed by infection of H5N1 with 10-fold dilution (MOI = 1). Total RNA was extracted from the cells at 0, 6, 12 and 24 hpi of H5N1 infection and reverse transcribed. Thereafter, the qPCR was performed using specific primer targeting M2 gene of H5N1. (A) A549, (B) MDCK.

3.2. Recombinant adenovirus can effectively express human IFITM3 in different cells

Total RNA was extracted from rAd5-IFITM3 or wtAd5 infected HEK293 cell, followed by reverse transcription using M-MLV reverse transcriptase. Thereafter, PCR was performed using primers IFITM3 as described previously. The results showed that human IFITM3 can be detected in rAd5-IFITM3-infected HEK293 cell, while no specific amplicon was detected in wtAd5-infected HEK293 cells (Fig. 3a). Furthermore, HEK293, MDCK and A549 cells were infected with rAd5-IFITM3 or wtAd5. 48 hpi, the cells were collected and processed by RIPA lysis buffer (Beyotime, China), followed by western blot analysis of human IFITM3. The results showed that obvious bands of human IFITM 3 can be examined in rAd5-IFITM3-infected HEK293, MDCK and A549 cells, but no band was detected in wtAd5-infected or mock cells (Fig. 3b).

Moreover, MDCK and A549 cells were infected with rAd5-IFITM3 or wtAd5. Total proteins were collected at 12, 24, 36 and 48 hpi, and examined using western blot. As shown in Fig. 4, obvious bands of human IFITM 3 can be examined in rAd5-IFITM3-infected MDCK and A549 cells at 12, 24, 36 and 48 hpi, but no band was detected in wtAd5-infected or mock cells. The expression of human IFITM3 was increased as time going on in these cells.

Additionally, distribution of human IFITM3 in MDCK and A549 cells were determined by western blot. The results demonstrated that majority of human IFITM3 were detected in cell membrane of the rAd5-IFITM3-infected cells, while no bands was detected in mock infected cells (Fig. 5). In addition, no band was detected in wtAd5-infected A549 and MDCK cells, except that a weak band was detected in cell membrane of the wtAd5-infected MDCK cell.
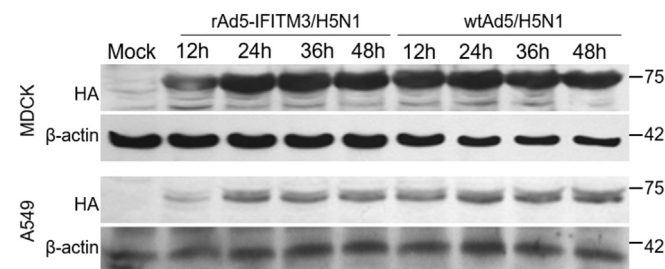
These results demonstrated that recombinant adenovirus can effectively express human IFITM3 in different cells. The human IFITM3 was mainly located on cell membrane, which was consistent with the result reported previously [31,32].

3.3. Human IFITM3 has no effect on recombinant adenovirus

To evaluate CPE of recombinant adenovirus on cells, A549 and MDCK cells were infected with rAd5-IFITM3 or wtAd5 at different MOI (1, 10, 100 and 1000). The inhibition rate of cell growth was calculated using MTS at 12, 24, 36 and 48 hpi. The results showed that both adenoviruses, including rAd5-IFITM3 and wtAd5, can induce CPE in MDCK and A549 cells in a dose and time dependent manner, while there was no significant difference of CPE between rAd5-IFITM3 and wtAd5 infected cells (Fig. 6), indicating human IFITM3 has no effect on recombinant adenovirus.

Furthermore, A549 and MDCK cells were infected with rAd5-IFITM3 or wtAd5 at MOI of 100. CPE was observed using microscope at 12, 24, 36, 48 and 72 hpi. The results showed that obvious CPE appeared at 48 and 72 hpi in rAd5-IFITM3-infected MDCK and A549 cells (Fig. 7). Based on these observations, cells infected with the recombinant adenovirus at an MOI of 100 for 24 h were selected for subsequent experiments.

3.4. Recombinant adenovirus expressing human IFITM3 can inhibit H5N1 infection in vitro

A549 and MDCK cells were infected with rAd5-IFITM3 or wtAd5 at an MOI of 100. 6, 12 and 24 hpi, expression levels of M2 gene of AIV H5N1 were evaluated by qPCR. The results showed that expression levels of M2 gene were significantly inhibited in rAd5-IFITM3-treated cell compared with that of wtAd5-treated cells and mock cells at 6, 12 and 24 hpi for A549 and at 6 and 12 hpi for MDCK cells (Fig. 8).

Moreover, level of HA protein of AIV H5N1 was examined using western blot. The results showed that HA protein of H5N1 was significantly decreased in rAd5-IFITM3-treated cell compared with that of wtAd5-treated cells at 12 hpi for A549 and MDCK cells (Fig. 9). However, no significant difference was observed between rAd5-IFITM3-treated cells and wtAd5-treated cells at 24, 36 and 48 hpi. These results suggested that IFITM3 inhibited influenza virus H5N1 in the early stage of the infection, which was consistent with the results reported previously [33,34].

Fig. 9. Western blot. MDCK (top panel) and A549 (bottom panel) cells were infected with rAd5-IFITM3 or wtAd5 at an MOI of 100 for 24 h, followed by infection of H5N1 with 10-fold dilution (MOI = 1). Total protein was extracted from the cells at 12, 24, 36 and 48 hpi of H5N1 infection. Mock infected cells were used as negative control. Thereafter, western blot was performed using Anti-HA antibody (1:1000, Proteintech, USA) or Mouse monoclonal anti-β-actin antibody (1:1000, Beyotime, China) as primary antibody and HRP-conjugated goat anti-mouse IgG as secondary antibody (1:2000, Beyotime, China).

4. Discussion

Currently, >20 types of interferon-stimulated genes (ISGs) have been discovered, which play antiviral role in different stages of virus life cycle by different mechanisms. Among ISGs, IFITM3 is one of the

most promising antiviral agents with better application prospect [18,35]. Firstly, IFITM3 has a broad-spectrum antiviral activity, which have been reported to inhibit entering of >20 kinds of viruses, including different subtypes of influenza virus, severe acute respiratory syndrome (SARS) coronavirus, human immunodeficiency virus (HIV), Ebola virus, dengue, and West Nile viruses and so on [26–30,35–37]. Secondly, to date, IFITM3 is the only ISG discovered displaying a *bona fide* role in blocking virus entry, to defense virus outside the cell. Thirdly, the antiviral activity of IFITM3, in particular, is high, with the inhibition rate is up to 70% for influenza virus [30,37]. Fourthly, to date, as an endogenous molecule, IFITM3 has no immunogenicity and toxic side effect to the host cells. Finally, its molecular weight is smaller, with 133 amino acids [35], as compared to other ISGs, and is easy to be studied and applied in gene therapy and vaccine development. However, whether IFITM3 can be used as antiviral drug is still unknown.

IFITM3 is a virus restriction factor which primarily localizes to endosomes and lysosomes [38]. Thus, a suitable vector or strategy is needed to transfer the protein into the target cell. Till now, adenovirus is one of the most effective means of delivering gene *in vitro* and *in vivo*, which have been widely used in therapies for cancer, high-level, short-term expression of the target gene for gene therapy, vaccine for infection disease [1,2,5,9–12,39–42]. In additionally, adenovirus vector is one of the most common vectors used in clinical trials, as human therapy studies based on adenovirus vector is up to 23.5% of all gene therapy trials worldwide [5]. Therefore, recombinant adenovirus was obtained by co-transfection of the linearized viral backbone vector pAd5 and the shuttle pacAd-IFITM3 containing human IFITM3 in the present study. The results showed that expression of IFITM3 did not affect the assembly and morphogenesis of progeny adenovirus, indicating that human IFITM3 has no effect on recombinant adenovirus (Figs. 2, 6 and 7). Furthermore, human IFITM3 expressed by the recombinant adenovirus was increased in a time dependent manner in the cells (Fig. 4). In addition, the recombinant adenovirus can effectively express human IFITM3 in both A549 and MDCK cells (Figs. 3 and 4). These results further confirmed that the recombinant adenovirus constructed in this study has a broad host range, which can be used in the future research and clinical practice.

However, in some circumstance, recombinant adenovirus or adenovirus vector can cause typical CPE on cells [5], as shown in Figs. 1c and 7, resulting in grape-like clusters of rounded, refractive cells, which appear in 3 to 10 days post-infection [43]. And, significant escalation in the dose of the recombinant adenovirus will increase the risk of inducing both direct toxicity and immune responses against the adenovirus [2]. Therefore, the MOI of rAd5-IFITM3 was determined by calculating the inhibition rate of the adenovirus on cell growth using MTS, and CPE was observed using microscopy. Based on the results in Figs. 4, 6 and 7, cells infected with the recombinant adenovirus at an MOI of 100 for 24 h were selected for subsequent experiments of H5N1 infection.

IFITM3 blocks virus fusion with cell membranes *via* acidic endosome [38,44]. According to the previous reports, the IFITM3 gene is conserved in chimpanzee, Rhesus monkey, mouse, and rat, and 14 organisms have orthologs with human IFITM3 gene (https://www.ncbi.nlm.nih.gov/gene/10410), indicating a cross protection between species was exist. In order to evaluate antiviral efficacy, both A549 and MDCK cells infected with rAd5-IFITM3 or wtAd5 at an MOI of 100 for 24 h were challenged with H5N1 at an MOI of 1. The results showed that the expressions of viral genes in rAd5-IFITM3-treated cells were significantly inhibited at transcriptional and translational levels than that of wtAd5-treated counterparts (Figs. 8 and 9), demonstrating that human IFITM3 can suppress AIV H5N1 infection in these cells. These results suggested that IFITM3 inhibited AIV H5N1 in the early stage of the infection, which was consistent with the results reported previously [32–34]. The *in vivo* utility of the present generation of rAd5-IFITM3 against H5N1 infection is in progress.

Moreover, we found that the human IFITM3 was mainly located on cell membrane (Fig. 5), which was consistent with the previously reports [31,32]. Surprisingly, a weak band was also detected in cellular membrane of the wtAd5-infected MDCK cell (Fig. 5). It was reported that adenovirus or adenovirus vector induced rapid and strong innate immune response which may shorten the duration of the gene therapy and vaccination [5,45,46]. Therefore, the possible reason was that IFN response was induce by adenovirus, resulting in expression of endogenous IFITM3 in cellular membrane of the wtAd5-infected MDCK cells. However, further study is needed to elucidate the mechanism involved.

5. Conclusions

In conclusion, we rescued a recombinant adenovirus rAd5-IFITM3 expressing human IFITM3. We also evaluated, for the first time, whether IFITM3 can be used in antiviral therapy. The results showed that the rAd5-IFITM3 can inhibit influenza virus H5N1 in the early stage of the infection, indicating that the rAd5-IFITM3 may be used as a promise agent against AIV H5N1 infection. The data in the present study may serve as a basis for *in vivo* studies and clinical utility of the recombinant adenovirus rAd5-IFITM3.

Ethics approval and consent to participate

All animal experimental protocols were approved by the Institutional Animal Care and Use Committee of the Military Veterinary Institute, Academy of Military Medical Science (10ZDGG007).

Availability of data and materials

The datasets used and/or analyzed during the current study are available from the corresponding author on reasonable request.

Conflict of interest statement

The authors declare that they have no competing interests.

Acknowledgments

References

[1] W.S.M. Wold, K. Toth, Adenovirus vectors for gene therapy, vaccination and cancer gene therapy, Curr Gene Ther 13 (6) (2013) 421–433.
[2] I. Dmitriev, V. Krasnykh, C.R. Miller, M. Wang, E. Kashentseva, G. Mikheeva, N. Belousova, D.T. Curiel, An adenovirus vector with genetically modified fibers demonstrates expanded tropism via utilization of a coxsackievirus and adenovirus receptor-independent cell entry mechanism, J. Virol. 72 (12) (1998) 9706–9713.
[3] M. Barry, Single-cycle adenovirus vectors in the current vaccine landscape, Expert Rev. Vaccines 17 (2) (2018) 163–173.
[4] A.A. Stepanenko, V.P. Chekhonin, A compendium of adenovirus genetic modifications for enhanced replication, oncolysis, and tumor immunosurveillance in cancer therapy, Gene 679 (2018) 11–18.
[5] R.G. Crystal, Adenovirus: the first effective in vivo gene delivery vector, Hum. Gene Ther. 25 (1) (2014) 3–11.
[6] R.J. Parks, F.L. Graham, A helper-dependent system for adenovirus vector production helps define a lower limit for efficient DNA packaging, J. Virol. 71 (4) (1997) 3293–3298.
[7] F.L. Graham, L. Prevec, Adenovirus-based expression vectors and recombinant vaccines, Biotechnology 20 (1992) 363–390.
[8] X.Y. Li, D.A. Drakulich, P.J. Zhang, M.L. Shen, G.A. Weber, T. Ikezu, T.D. Hexum, Transduction of bovine adrenal chromaffin cells using a recombinant adenovirus expressing GFP, J. Neurosci. Methods 122 (1) (2002) 91–96.
[9] V. Martin, E. Pascual, M. Avia, G. Rangel, A. de Molina, A. Alejo, N. Sevilla, A recombinant adenovirus expressing ovine interferon tau prevents influenza virus-induced lethality in mice, J. Virol. 90 (7) (2016) 3783–3788.
[10] E.S. Gabitzsch, J.P. Balint-Junior, Y. Xu, S. Balcaitis, B. Sanders-Beer, J. Karl, K.J. Weinhold, S. Paessler, F.R. Jones, Control of SIV infection and subsequent induction

of pandemic H1N1 immunity in rhesus macaques using an Ad5 [E1-, E2b-] vector platform, Vaccine 30 (50) (2012) 7265–7270.

[11] W.G. Tan, I. Zubkova, A. Kachko, F. Wells, H. Adler, G. Sutter, M.E. Major, Qualitative differences in cellular immunogenicity elicited by hepatitis C virus T-Cell vaccines employing prime-boost regimens, PLoS One 12 (7) (2017), e0181578.

[12] A. Benlahrech, J. Harris, A. Meiser, T. Papagatsias, J. Hornig, P. Hayes, A. Lieber, T. Athanasopoulos, V. Bachy, E. Csomor, R. Daniels, K. Fisher, F. Gotch, L. Seymour, K. Logan, R. Barbagallo, L. Klavinskis, G. Dickson, S. Patterson, Adenovirus vector vaccination induces expansion of memory CD4 T cells with a mucosal homing phenotype that are readily susceptible to HIV-1, Proc. Natl. Acad. Sci. U. S. A. 106 (47) (2009) 19940–19945.

[13] C.C. Bailey, H.R. Kondur, I.C. Huang, M. Farzan, Interferon-induced transmembrane protein 3 is a type II transmembrane protein, J. Biol. Chem. 288 (45) (2013) 32184–32193.

[14] K. Li, R.M. Markosyan, Y.M. Zheng, O. Golfetto, B. Bungart, M. Li, S. Ding, Y. He, C. Liang, J.C. Lee, E. Gratton, F.S. Cohen, S.L. Liu, IFITM proteins restrict viral membrane hemifusion, PLoS Pathog. 9 (1) (2013), e1003124.

[15] A.M. Sällman, N. Bringeland, R. Fredriksson, H.B. Schiöth, The dispanins: a novel gene family of ancient origin that contains 14 human members, PLoS One 7 (2) (2012), e31961.

[16] D. Hickford, S. Frankenberg, G. Shaw, M.B. Renfree, Evolution of vertebrate interferon inducible transmembrane proteins, BMC Genomics 13 (2012) 155.

[17] S.K. Narayana, K.J. Helbig, E.M. McCartney, N.S. Eyre, R.A. Bull, A. Eltahla, A.R. Lloyd, M.R. Beard, The interferon-induced transmembrane proteins, IFITM1, IFITM2, and IFITM3 inhibit hepatitis C virus entry, J. Biol. Chem. 290 (43) (2015) 25946–25959.

[18] J. Zhang, Z. Liu, Y. Zou, N. Zhang, D. Wang, D. Tu, L. Yang, Z. Deng, Y. Yang, P. Jiang, N. Wang, First molecular detection of porcine circovirus type 3 in dogs in China, Virus Genes 54 (1) (2018) 140–144.

[19] G. Savidis, J.M. Perreira, J.M. Portmann, P. Meraner, Z.R. Guo, S. Green, A.L. Brass, The IFITMs inhibit Zika virus replication, Cell Rep. 15 (11) (2016) 2323–2330.

[20] S. Weston, S. Czieso, I.J. White, S.E. Smith, R.S. Wash, C. Diaz-Soria, P. Kellam, M. Marsh, Alphavirus restriction by IFITM proteins, Traffic 17 (9) (2016) 997–1013.

[21] X. Zhao, M. Sehgal, Z. Hou, J. Cheng, S. Shu, S. Wu, F. Guo, S.J. Le Marchand, H. Lin, J. Chang, J.T. Guo, Identification of residues controlling restriction versus enhancing activities of IFITM proteins on entry of human coronaviruses, J. Virol. 92 (6) (2018).

[22] J. Wilkins, Y.M. Zheng, J. Yu, C. Liang, S.L. Liu, Nonhuman primate IFITM proteins are potent inhibitors of HIV and SIV, PLoS One 11 (6) (2016), e0156739.

[23] Y. Jiang, S. Du, T. Cao, F. Zhao, M. Wang, P. Tan, S. Xin, Y. Zhu, W. Li, Y. Li, T. Li, C. Li, N. Jin, Establishment of A549 cell stain stably expressing human IFITM3 and its inhibition to avian influenza virus infection, Chin. J. Immunol. 32 (3) (2016) 372–376.

[24] G. Shi, O. Schwartz, A.A. Compton, More than meets the I: the diverse antiviral and cellular functions of interferon-induced transmembrane proteins, Retrovirology 14 (1) (2017) 53.

[25] A.A. Compton, N. Roy, F. Porrot, A. Billet, N. Casartelli, J.S. Yount, C. Liang, O. Schwartz, Natural mutations in IFITM3 modulate post-translational regulation and toggle antiviral specificity, EMBO Rep. 17 (11) (2016) 1657–1671.

[26] A.L. Brass, I.C. Huang, Y. Benita, S.P. John, M.N. Krishnan, E.M. Feeley, B.J. Ryan, J.L. Weyer, L. van der Weyden, E. Fikrig, The IFITM proteins mediate cellular resistance to influenza A H1N1 virus, West Nile virus, and dengue virus, Cell 139 (7) (2009) 1243–1254.

[27] C.C. Bailey, G. Zhong, I.C. Huang, M. Farzan, IFITM-family proteins: the cell's first line of antiviral defense, Annu. Rev. Virol. 1 (2014) 261–283.

[28] J.S. Spence, R. He, H.H. Hoffmann, T. Das, E. Thinon, C.M. Rice, T. Peng, K. Chandran, H.C. Hang, IFITM3 directly engages and shuttles incoming virus particles to lysosomes, Nat. Chem. Biol. 15 (3) (2019) 259–268, https://doi.org/10.1038/s41589-018-0213-2.

[29] B. Monel, A.A. Compton, T. Bruel, S. Amraoui, J. Burlaud-Gaillard, N. Roy, F. Guivel-Benhassine, F. Porrot, P. Genin, L. Meertens, L. Sinigaglia, N. Jouvenet, R. Weil, N. Casartelli, C. Demangel, E. Simon-Loriere, A. Moris, P. Roingeard, A. Amara, O. Schwartz, Zika virus induces massive cytoplasmic vacuolization and paraptosis-like death in infected cells, EMBO J. 36 (12) (2017) 1653–1668.

[30] S. Smith, S. Weston, P. Kellam, M. Marsh, IFITM proteins-cellular inhibitors of viral entry, Curr. Opin. Virol. 4 (2014) 71–77.

[31] A.R. Everitt, S. Clare, T. Pertel, S.P. John, R.S. Wash, S.E. Smith, C.R. Chin, E.M. Feeley, J.S. Sims, D.J. Adams, H.M. Wise, L. Kane, D. Goulding, P. Digard, V. Anttila, J.K. Baillie, T.S. Walsh, D.A. Hume, A. Palotie, Y. Xue, V. Colonna, C. Tyler-Smith, J. Dunning, S.B. Gordon, I.I. Gen, M. Investigators, R.L. Smyth, P.J. Openshaw, G. Dougan, A.L. Brass, P. Kellam, IFITM3 restricts the morbidity and mortality associated with influenza, Nature 484 (7395) (2012) 519–523.

[32] S. Poddar, J.L. Hyde, M.J. Gorman, M. Farzan, M.S. Diamond, The interferon-stimulated gene IFITM3 restricts infection and pathogenesis of arthritogenic and encephalitic alphaviruses, J. Virol. 90 (19) (2016) 8780–8794.

[33] E.M. Feeley, J.S. Sims, S.P. John, C.R. Chin, T. Pertel, L.M. Chen, G.D. Gaiha, B.J. Ryan, R.O. Donis, S.J. Elledge, A.L. Brass, IFITM3 inhibits influenza A virus infection by preventing cytosolic entry, PLoS Pathog. 7 (10) (2011), e1002337.

[34] J. Xu, P. Qian, Q. Wu, S. Liu, W. Fan, K. Zhang, R. Wang, H. Zhang, H. Chen, X. Li, Swine interferon-induced transmembrane protein, sIFITM3, inhibits foot-and-mouth disease virus infection in vitro and in vivo, Antivir. Res. 109 (2014) 22–29.

[35] M.S. Diamond, M. Farzan, The broad-spectrum antiviral functions of IFIT and IFITM proteins, Nat. Rev. Immunol. 13 (1) (2013) 46–57.

[36] C. Li, H. Zheng, Y. Wang, W. Dong, Y. Liu, L. Zhang, Y. Zhang, Antiviral Role of IFITM Proteins in Classical Swine Fever Virus Infection, Viruses 11 (2) (2019)https://doi.org/10.3390/v11020126 pii: E126.

[37] J.M. Perreira, C.R. Chin, E.M. Feeley, A.L. Brass, IFITMs restrict the replication of multiple pathogenic viruses, J. Mol. Biol. 425 (24) (2013) 4937–4955.

[38] N.M. Chesarino, A.A. Compton, T.M. McMichael, A.D. Kenney, L. Zhang, V. Soewarna, M. Davis, O. Schwartz, J.S. Yount, IFITM3 requires an amphipathic helix for antiviral activity, EMBO Rep. 18 (10) (2017) 1740–1751.

[39] B.L. Bullard, B.N. Corder, M.J. Gorman, M.S. Diamond, E.A. Weaver, Efficacy of a T cell-biased adenovirus vector as a Zika virus vaccine, Sci. Rep. 8 (1) (2018), 18017.

[40] S.W. Du, C.X. Liu, Y.L. Zhu, Y.H. Wang, D.Y. Ren, M.P. Wang, P. Tan, X. Li, M.Y. Tian, Y.F. Zhang, J.Z. Li, F. Zhao, C. Liu, N.Y. Jin, Construction and characterization of novel fowlpox virus shuttle vectors, Virus Res. 197 (2015) 59–66.

[41] R.E. Tamura, I.V. de Luna, M.G. Lana, B.E. Strauss, Improving adenoviral vectors and strategies for prostate cancer gene therapy, Clinics (Sao Paulo) 73 (Suppl. 1) (2018) e476s.

[42] M.D. Baron, M. Iqbal, V. Nair, Recent advances in viral vectors in veterinary vaccinology, Curr. Opin. Virol. 29 (2018) 1–7.

[43] J.A. Armstrong, H.G. Pereira, Significance of cytopathic effects observed during the growth of adenovirus, Exp. Cell Res. 21 (1960) 144–150.

[44] Y.H. Zhang, Y. Zhao, N. Li, Y.C. Peng, E. Giannoulatou, R.H. Jin, H.P. Yan, H. Wu, J.H. Liu, N. Liu, D.Y. Wang, Y.L. Shu, L.P. Ho, P. Kellam, A. McMichael, T. Dong, Interferon-induced transmembrane protein-3 genetic variant rs12252-C is associated with severe influenza in Chinese individuals, Nat. Commun. 4 (2013).

[45] M. Machitani, T. Yamaguchi, K. Shimizu, F. Sakurai, K. Katayama, K. Kawabata, H. Mizuguchi, Adenovirus vector-derived VA-RNA-mediated innate immune responses, Pharmaceutics 3 (3) (2011) 338–353.

[46] Z.C. Hartman, D.M. Appledorn, A. Amalfitano, Adenovirus vector induced innate immune responses: impact upon efficacy and toxicity in gene therapy and vaccine applications, Virus Res. 132 (1–2) (2008) 1–14.